Single Pulse Phase-Control Interferometric Coherent anti-Stokes Raman Scattering Spectroscopy (CARS)

Sang-Hyun Lim, Allison G. Caster and Stephen R. Leone

Departments of Chemistry and Physics, University of California at Berkeley and Lawrence Berkeley National Laboratory, Berkeley, California, 94720, U.S.A.

Abstract

In coherent anti-Stokes Raman scattering spectroscopy (CARS) experiments, usually the amplitude of the signal is measured and the phase information is lost. With a polarization- and phase-controlled pulse shaping technique, the relative phase between the resonant and non-resonant CARS signals is controlled, and spectral interferometry is performed without an interferometer. Both the real and imaginary parts of the background-free resonant CARS spectrum are measured via spectral interferometry between the resonant and non-resonant signals from the same sample. The resonant signal is amplified significantly by homodyne mixing with the non-resonant signal as a local oscillator, greatly improving the detection limit.

Coherent anti-Stokes Raman scattering (CARS) spectroscopy has emerged as a promising microscopic technique for materials and biological imaging [1,2]. Optical molecular imaging is often limited by the necessary introduction of dyes or markers, which can perturb material structures or alter biological processes. Since CARS allows the identification of the desired molecules by their vibrational response, it circumvents the need for fluorescent labels [1,3,4].

In this letter, we demonstrate that it is possible to retrieve the imaginary part of the background-free resonant CARS spectrum *in situ* via spectral interferometry utilizing the non-resonant signal from the same sample as a local oscillator. We apply the polarization- and phase-control pulse shaping technique [5] to control the relative phase between the resonant and non-resonant CARS signal [6,7], but implement a double quadrature spectral interferometry (DQSI) method [8] utilizing the non-resonant signal as a local oscillator. Unlike previously reported interferometric CARS techniques [9,10], the interference between the two signals (the resonant and non-resonant CARS) is produced in the same sample, and the imaginary part of the resonant CARS spectrum is acquired directly. The technique not only extracts the imaginary part of the CARS signal, but also amplifies it significantly, allowing a further sensitivity improvement [9].

Most non-linear spectroscopy experiments measure only the amplitude of a spectral response and CARS is similar [11]. Fig. 1(a) shows the square of the amplitude ($|L|^2$, the conventional CARS signal), and the imaginary (*Im*[*L*]) and real (*Re*[*L*]) parts of several Lorentzian lines (*L*) simulated for toluene [12].

$$L(\omega) = \sum_k \frac{A_k}{\omega - \Omega_k - i\Gamma_k} \tag{1}$$

where A_k, Ω_k and Γ_k are the intensity, energy and linewidth of the vibrational mode *k*, respectively. The imaginary part of the vibrationally resonant third order non-linear susceptibility $\chi_{res}^{(3)}$ corresponds to the spontaneous Raman spectrum [9]. Although $|L|^2$ has a comparable spectral resolution to *Im*[*L*], its spectral intensity distribution and the detailed peak shapes are different from *Im*[*L*] [9].

It is desirable to measure *Im*[*L*], which correlates directly with the wealth of vibrational Raman information available [12,13]. Detecting $|L|^2$ has additional problems because of non-resonant signals, which dominate most condensed phase samples [1,3,14]. Since both the resonant and non-resonant signals are coherent, the two components interfere with each other, generating a modulated pattern in the measured CARS spectrum, which makes it difficult to use assignments from the known Raman spectrum directly (the interference pattern resembles the shape of *Re*[*L*] shown in Fig. 1(a)) [1,14].

With single broad band pulse excitation, all possible combinations of wavelengths within the bandwidth can be used as pump, Stokes and probe pulses to generate the CARS signal (Fig. 1(b)). The resonant and non-resonant CARS signals can be described by [6]

$$P_R(\omega) \propto \int_0^\infty d\Omega \frac{1}{(\Omega_R - \Omega) + i\Gamma_R} E(\omega - \Omega) A(\Omega) \tag{1}$$

$$P_{NR}(\omega) \propto \int_0^\infty d\Omega \frac{1}{\Omega} E(\omega - \Omega) A(\Omega) \tag{2}$$

where $$A(\Omega) = \int_0^\infty d\omega' E^*(\omega') E(\Omega + \omega') \tag{3}$$

P_R and P_{NR} are the vibrationally resonant and the non-resonant polarizations, respectively, E is the laser field, and Ω_R and Γ_R represent the energy and the linewidth of the vibrational resonance, respectively. Note that P_{NR} is real and P_R is complex [6]. To obtain a multiplex CARS signal, it is necessary to separate a spectrally narrow probe pulse, and Silberberg and co-workers demonstrated this by applying phase- and polarization-control techniques [6,7]. If we assume that the linewidth of the probe (selected by the phase and polarization as shown in Fig. 2(a)) is spectrally much narrower than the linewidth of the vibrational peak (Γ_R), the resonant CARS component becomes

$$
\begin{aligned}
P_R(\omega) &\propto \int_0^\infty d\Omega \frac{1}{(\Omega_R - \Omega) + i\Gamma_R} E_{\mathrm{Pr}}(\omega - \Omega) A(\Omega) \\
&\approx \int_0^\infty d\Omega \frac{1}{(\Omega_R - \Omega) + i\Gamma_R} \delta(\omega - \Omega - \omega_{\mathrm{Pr}}) \exp(i\phi_{\mathrm{Pr}}) A(\Omega) \\
&= \frac{\exp(i\phi_{\mathrm{Pr}})}{\Omega_R + \omega_{\mathrm{Pr}} - \omega + i\Gamma_R} A(\omega - \omega_{\mathrm{Pr}}) = L(\omega) \exp(i\phi_{\mathrm{Pr}}) A(\omega - \omega_{\mathrm{Pr}})
\end{aligned}
\qquad (4)
$$

if $E_{Pr}(\omega) \approx \delta(\omega - \omega_{Pr}) exp(i\phi_{Pr})$

where L is the Lorentzian line shape function for CARS (the only difference from Eq. (1) is the relative resonance energy, i.e. $\Omega_R + \omega_R$ instead of Ω_R), δ is the delta function, ϕ_{Pr} is the relative phase of the probe with respect to the excitation part of the pulse (as shown in Fig. 2(a)), and ω_{Pr} is the frequency of the probe pulse.

The experimental scheme is shown in Fig. 2. Fig. 2(a) shows the intensity, phase and polarization of the laser pulse controlled by the pulse shaper. Polarizations of the pump/Stokes and the probe pulses are along the x- and y-directions, respectively, as shown in Fig. 2(b). If we detect CARS signals along the ±45º polarization directions relative to the x-axis (i- and j-directions in Fig. 2(b)), the CARS polarizations in the i- and j-polarization directions are

$$P_R^i = \frac{1}{\sqrt{2}} exp(i\phi_{Pr})AL \;,\; P_R^j = -\frac{1}{\sqrt{2}} exp(i\phi_{Pr})AL \;,\; P_{NR}^i = P_{NR}^j = \frac{1}{\sqrt{2}} P_{NR} \qquad (5)$$

The detected signals (S^i and S^j) become

$$\begin{aligned} S^i &= \left|\alpha_R P_R^i + \alpha_{NR} P_{NR}^i\right|^2 = \alpha_R^2 \left|P_R^i\right|^2 + \frac{1}{2}\alpha_{NR}^2 \left|P_{NR}\right|^2 + \frac{1}{\sqrt{2}}\alpha_R \alpha_{NR}(P_R^i + P_R^{i*})P_{NR}, \\ S^j &= \left|\alpha_R P_R^j + \alpha_{NR} P_{NR}^j\right|^2 = \alpha_R^2 \left|P_R^j\right|^2 + \frac{1}{2}\alpha_{NR}^2 \left|P_{NR}\right|^2 + \frac{1}{\sqrt{2}}\alpha_R \alpha_{NR}(P_R^j + P_R^{j*})P_{NR} \end{aligned} \qquad (6)$$

where α_{NR} and α_R are the intensity coefficients for the non-resonant and resonant CARS polarizations, respectively. Here we limit the consideration to randomly oriented samples. Since only a small portion of the laser spectrum is used as a probe (2 pixels out of 128 SLM pixels), we assume that P_{NR} is primarily parallel to the x-axis (pump/Stokes direction). Combining Eq. (5) and Eq. (6), we find that the difference, S^i - S^j, becomes

$$\begin{aligned} S^i - S^j &= \alpha_R \alpha_{NR} \frac{P_{NR}}{\sqrt{2}} (P_R^i + P_R^{i*} - P_R^j - P_R^{j*}) \\ &= \alpha_R \alpha_{NR} P_{NR} A\left\{\exp(i\phi_{\mathrm{Pr}})L + \exp(-i\phi_{\mathrm{Pr}})L^*\right\} \\ &= \alpha_R \alpha_{NR} P_{NR} A\left\{e^{i\phi_{\mathrm{Pr}}}(\mathrm{Re}[L] + i\,\mathrm{Im}[L]) + e^{-i\phi_{\mathrm{Pr}}}(\mathrm{Re}[L] - i\,\mathrm{Im}[L])\right\} \\ &= 2\alpha_R \alpha_{NR} P_{NR} A(\mathrm{Re}[L]\cos\phi_{\mathrm{Pr}} - \mathrm{Im}[L]\sin\phi_{\mathrm{Pr}}) \end{aligned} \qquad (7)$$

where *Re[L]* and *Im[L]* represent the real and imaginary parts of the Lorentzian line shape function, respectively. Eq. (7) means that if we can detect S^i and S^j simultaneously, the real or imaginary parts of the resonant CARS signal (L) can be extracted simply by controlling the phase of the probe pulse (ϕ_{Pr} in Fig. 2(a)). Since $S^i + S^j$ contains mostly non-resonant signals, we can extract the non-amplified resonant signal by the following normalized difference (D),

$$D = \frac{S^i - S^j}{\sqrt{S^i + S^j}} = \frac{2\alpha_{NR}\alpha_R P_{NR} A \,\mathrm{Im}[L]}{\sqrt{\alpha_{NR}^2 P_{NR}^2 + \frac{1}{2}(\alpha_R^2 \left|P_R^i\right|^2 + \alpha_R^2 \left|P_R^j\right|^2) + cross\ terms}} \approx 2\alpha_R A \,\mathrm{Im}[L] \quad (8)$$

In this way, we can detect only the resonant signals from samples that have different levels of non-resonant signals.

In the experimental setup (Fig. 2(c)), we control the phase and polarization of the laser pulse by an all-reflective 4*f* geometry pulse shaper with a dual 128 pixel liquid crystal spatial light modulator (LC-SLM, SLM-256, CRI) [5,7]. We compress the pulse at the sample position with a multiphoton intrapulse interference phase scan (MIIPS)[15]. To obtain an optimum CARS signal level, it is also necessary to compress the higher order chirp, not just the quadratic phase modulation terms. Dispersion induced by most samples is negligible due to the short working distance (280 μm) of the microscope objective used in this experiment. After generating and collecting the CARS signal with microscope objectives (1.2 NA and 1.0 NA, respectively, IR water immersion objectives, Olympus), the polarization is rotated by 45º with a Fresnel rhomb (achromatic half wave plate), and the i- and j-polarization signals are separated by a Wollaston prism. Directing the split beams (the i- and j-polarization signals) into an imaging spectrometer and onto a two dimensional CCD, we obtain both signal traces on every pulse [8,9,16]. The actual probe spectral linewidth in the experiment (30 cm^{-1}, corresponding to two pixels in the SLM) is wider than the Raman linewidth (~10 cm^{-1}), so Eq. (7) needs to be convoluted with the probe width. Note that we can simulate the experiment without the assumption of the narrow probe spectral width (Eq. (4)) by using the entire laser pulse spectrum in Eq. (2). However, we find that the general features are the same [16].

Fig. 3 shows the experimental signal spectra along the i- and j-directions (Figs. 3(a) and 3(b)) and the normalized difference spectra according to Eq. (8) (Fig. 3(c) and 3(d)) with two different probe phases. As one would expect from Eq. (7), with $\phi_{Pr} = -\pi/2$ the normalized difference signal (D) yields the imaginary part of the vibrational spectrum (Fig. 3(c)) and with $\phi_{Pr} = 0$, the real part is obtained (Fig. 3(d)). Note the similarity of Figs. 3(c) and 3(d) with the $Im[L]$ and $Re[L]$, respectively, shown in Fig. 1(a). As noted, the *Im[L]* is what corresponds to the Raman signal [9].

Fig. 4(a) shows the experimental DQSI-CARS spectra of several common lab solvents taken in a data acquisition time of 10 ms. The measured average laser power is 40 mW just before the focusing microscope objective. The laser repetition rate is 90 MHz, and the estimated peak power is ~2 x 10^{13} W/cm^2 at the focus. A small drop of the sample is sandwiched between two microscope coverslips. The currently accessible CARS window is from 400 to 1500 cm^{-1}, although the signal decreases rapidly beyond 1200 cm^{-1}. The spectral resolution is around 35 cm^{-1}, which is a little broader than the two pixel width of the SLM (30 cm^{-1}) that defines the probe width (Fig. 2(a)).

Detecting the cross term, $P_{NR}(P_R^* + P_R)$ in Eq. (6), instead of $|P_R|^2$, has two other advantages for the interferometric retrieval of the complex spectral line shape function. First, P_R is amplified with the help of the much bigger P_{NR}, so-called homodyne amplification [6,17]. Second, the signal depends linearly on the sample concentration instead of quadratically [9]; a quadratic sample concentration dependence is the case for the normal CARS signal [1]. The linear concentration dependence is an important benefit, since it makes additional experimental improvements easier. For example, if one wishes

to detect a sample at 10 times lower concentration, only 10 times better S/N is necessary, rather than 100.

Figs. 4(b) and (c) demonstrate the homodyne amplification advantage that our DQSI-CARS technique provides. The sample is 1M KNO_3 solution in water, which has a very weak CARS signal with a CCD exposure time of 10 ms. The same laser power as in Fig. 4(a) is used. We estimate the number of molecules in the excitation volume (~ 40 aL) is around 40 attomoles. Fig 4(b) shows a spectrum taken in a similar fashion to the phase- and polarization-controlled CARS method reported by Silberberg and co-workers [7]. In this technique, the non-resonant signal is blocked by a polarizer and only the resonant signal is measured. In Fig 4(c), the spectrum is taken by the DQSI-CARS technique with exactly the same experimental conditions (the same laser power and the same sample). Here we plot the difference between the signal traces (S^i - S^j) to directly compare the signal levels with the one in Fig 4 (b). As one can see in Figs 4(b) and (c), the resonant signal is amplified by ~100 times. At the vibrational frequency of 1025 cm^{-1}, the S^i and S^j have signal intensities of ~13000 counts. This corresponds to a local oscillator of ~110 $\sqrt{Counts}$ and the amplification of the resonant signal matches well with the theoretical expectation. One disadvantage of our technique is that the signal is accompanied by shot noise originating from the non-resonant signals. With strong CARS-signal samples such as toluene, the signal-to-noise ratio (S/N) is slightly worse compared to Silberberg's original technique. However, for weak signal samples, our technique shows much better sensitivity as demonstrated in Figs. 4 (b) and (c).

We also observed that the original phase- and polarization-controlled CARS method exhibits a problem with depolarization by the samples and optical components.

Even if a small amount of the signal is depolarized, the resonant signal is dominated by the leakage of the non-resonant background, which can be bigger by orders of magnitude. The shot noise from this background will obscure the weak resonant signal. In our technique, the depolarization will also distort the vibrational peak shapes and change the base line level. Nevertheless, the noise level will be the same and make no change in the S/N ratio. So the DQSI-CARS method is more tolerant to sample depolarization.

One important question is how pure is the phase of the local oscillator and how it affects the interferometric modulations. Here the non-resonant and resonant signals generated by the pump/Stokes part of the pulse (Fig. 2(a)) serve as the local oscillator, which is the large broad component in Figs. 3(a) and 3(b). If the local oscillator contains a significant amount of a resonant signal generated from the pump/Stokes part of the pulse, the interferometry will be contaminated by this sample-specific resonant signal. The relative ratio between P_R and P_{NR}, at 788 and 1008 cm^{-1}, is approximately 10% for toluene (Fig 3(a)). $\alpha_{NR}/\alpha_R = 500$ is required in Eqs. (6)-(8) to produce this amount of modulation. In most biological samples, this ratio will be significantly bigger by at least an order of magnitude because the resonant signal from the sample is small compared to the non-resonant signal from the solvent (water in most cases). From a numerical simulation with different values of α_{NR}/α_R, we find that even in the case of 10% modulation, the interferometry works reasonably well [16]. Even if the assumptions in Eq. (8) would break down in an extreme case, the result would be to distort the spectral shape, which would appear as a mixture of the imaginary and real parts, similar to previous

multiplex CARS experiments[18]. Still, the position and amplitude of the vibrational peaks could be extracted by a numerical fitting process [18].

In conclusion, we demonstrate that it is possible to do full spectral interferometry with the resonant and non-resonant CARS signals generated from a single sample without a conventional interferometry setup. By combining the single pulse CARS and the DQSI techniques, we are able to retrieve the imaginary part of the resonant CARS spectra over the entire accessible multiplex CARS window. This novel technique connects the measured CARS spectrum directly to the Raman counterpart and also improves the signal sensitivity of multiplex CARS spectroscopy.

Acknowledgement

The authors gratefully acknowledge the Department of Energy (Contract No. DE-AC03-76SF00098) for the instrumentation used in this research and the National Science Foundation, Division of Materials Research, for support of personnel. AGC acknowledges support of a National Science Foundation Graduate Fellowship.

References

[1] J. X. Cheng and X. S. Xie, J. Phys. Chem. B **108**, 827 (2004).

[2] E. O. Potma, X. S. Xie, L. Muntean, et al., J. Phys. Chem. B **108**, 1296 (2004).

[3] M. Muller and J. M. Schins, J. Phys. Chem. B **106**, 3715 (2002).

[4] N. Dudovich, D. Oron, and Y. Silberberg, Nature **418**, 523 (2002).

[5] T. Brixner and G. Gerber, Opt. Lett. **26**, 557 (2001).

[6] D. Oron, N. Dudovich, and Y. Silberberg, Phys. Rev. Lett. **89**, 273001 (2002).

[7] D. Oron, N. Dudovich, and Y. Silberberg, Phys. Rev. Lett. **90**, 213902 (2003).

[8] L. Lepetit, G. Cheriaux, and M. Joffre, J. Opt. Soc. Am. B **12**, 2467 (1995).

[9] C. L. Evans, E. O. Potma, and X. S. Xie, Opt. Lett. **29**, 2923 (2004).

[10] D. L. Marks, C. Vinegoni, J. S. Bredfeldt, et al., App. Phys. Lett. **85**, 5787 (2004).

[11] M. D. Levenson and S. S. Kano,*Introduction to Nonlinear spectroscopy* (Academic Press San Diego, 1988).

[12] F. R. Dollish, W. G. Fateley, and F. F. Bentley,*Characteristic Raman frequencies of organic compounds* (Johnson Willey and Sons New York, 1974).

[13] D. Lin-Vien, N. B. Colthup, W. G. Fateley, et al.,*The Handbook of Infrared and Raman Characteristic Frequencies of Organic Molecules* (Academic Press San Diego, 1991).

[14] J. X. Cheng, A. Volkmer, L. D. Book, et al., J. Phys. Chem. B **106**, 8493 (2002).

[15] V. V. Lozovoy, I. Pastirk, and M. Dantus, Opt. Lett. **29**, 775 (2004).

[16] S.-H. Lim, A. G. Caster, and S. R. Leone, in preparation (2005).

[17] Some authors refer to this as a heterodyne amplification. In our terminology, homodyne and heterodyne are with respect to the frequencies of the signal and local oscillator. Here the signal and local oscillator have the same frequencies and we use "homodyne" instead of heterodyne.

[18] G. W. H. Wurpel, J. M. Schins, and M. Muller, J. Phys. Chem. B **108**, 3400 (2004).

Figure Captions

Fig. 1. (a) Simulation of a Lorentzian line shape function of toluene (resonances at 788, 1001, 1028 and 1210 cm^{-1}) with Γ = 10 cm^{-1} in Eq. (1). Note that the spontaneous Raman spectrum corresponds to *Im*[*L*]. b) Energy level diagram of the CARS process.

Fig. 2. (a) Intensity, phase and polarization of the phase- and polarization-controlled laser pulse used in the experiment. (b) Polarization directions of pump/Stokes, probe and CARS signal detection (i and j). (c) Experimental setup. SLM – dual liquid crystal spatial light modulator, OBJ – microscope objective, S – sample, FR – Fresnel rhomb (achromatic half wave plate), SWP – sharp-edge short wave pass filter, WP – Wollaston prism, IS – imaging spectrometer.

Fig. 3. DQSI-CARS of toluene: (a), (b) The spectra in each polarization direction (i and j as in Fig. 2(b)) taken simultaneously in the imaging spectrometer. c), d) the normalized difference spectra (*D*) according to Eq. (8). (a), (c) are taken with $\phi_{probe} = -\pi/2$. (b), (d) with $\phi_{probe} = 0$, respectively. Note that (c) and (d) correspond to the imaginary and real parts of the resonant CARS spectrum.

Fig. 4. (a) Experimental DQSI-CARS spectra of common lab solvents. The data are taken with the microscope setup in 10 ms experiment times. (b),(c) Comparison of signal levels by the resonant-only CARS method and the homodyne-amplified DQSI-CARS method. (b) the phase- and polarization-controlled method according to Ref. 7. (c) DQSI method under the same experimental conditions. The sample is 1M KNO_3 solution in water and the experimental times are 10 ms. Note that this sample has ~ 40 times lower signal than toluene.

Fig.1

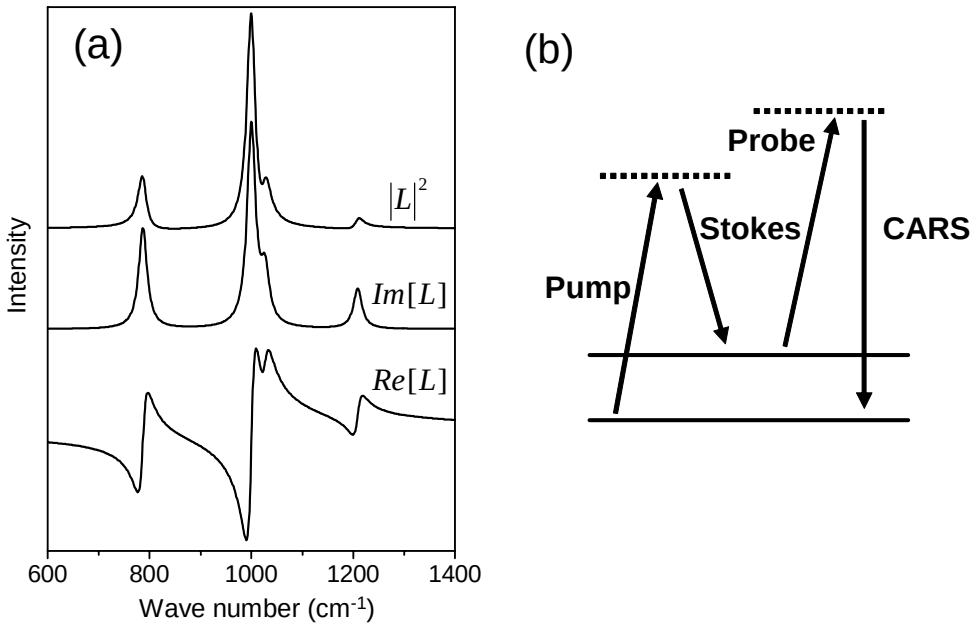
(a)
$|L|^2$
$Im[L]$
$Re[L]$
Intensity
600
800
1000
1200
1400
Wave number (cm-1)
(b)
Probe
Stokes
CARS
Pump

Fig.2

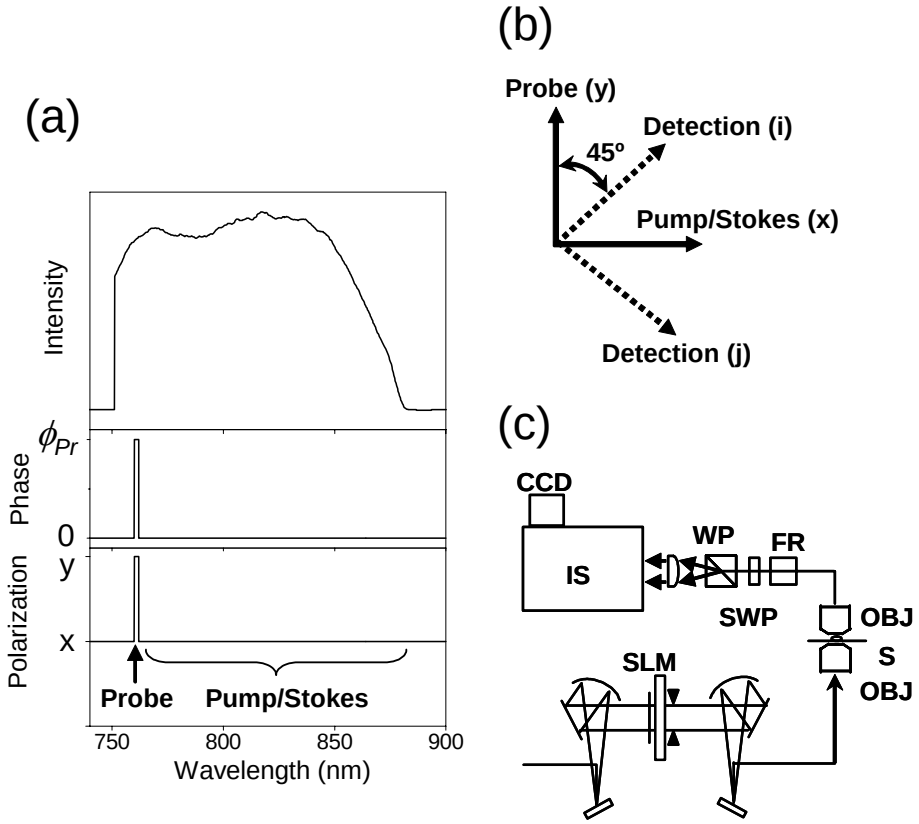
(a)
Intensity
Phase
ϕ_{Pr}
0
Polarization
y
x
Probe
Pump/Stokes
750
800
850
900
Wavelength (nm)
(b)
Probe (y)
Detection (i)
45°
Pump/Stokes (x)
Detection (j)
(c)
CCD
IS
WP
FR
SWP
OBJ
S
OBJ
SLM

Fig.3

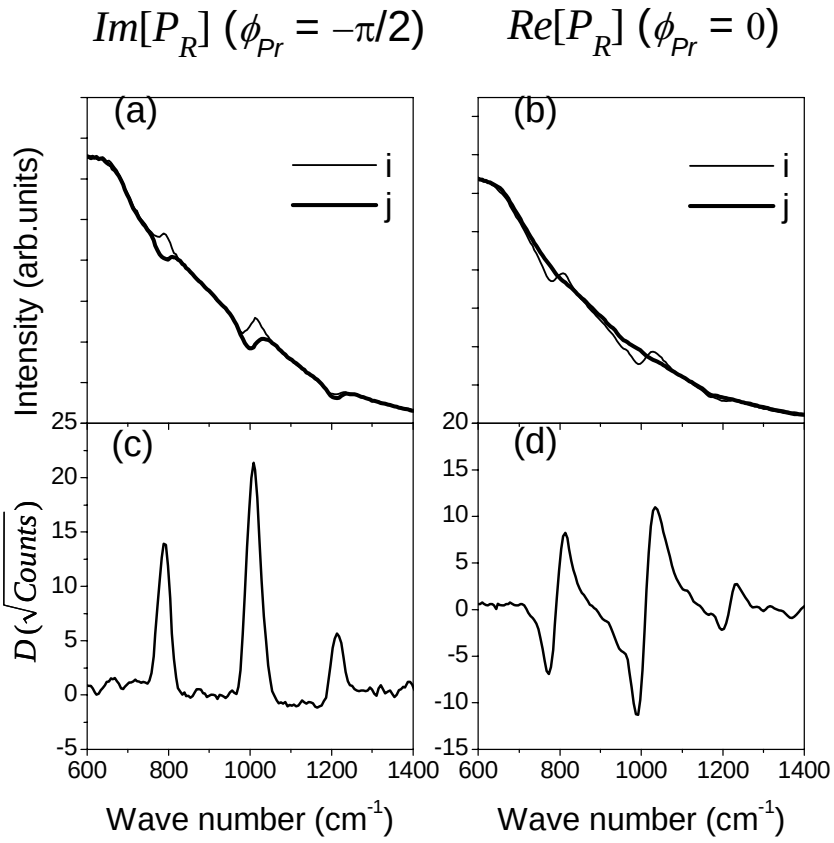
$Im[P_R]$ (ϕ_{Pr} = –π/2)
$Re[P_R]$ (ϕ_{Pr} = 0)
(a)
(b)
(c)
(d)
i
j
Intensity (arb.units)
$D(\sqrt{Counts})$
Wave number (cm^{-1})
Wave number (cm^{-1})

Fig.4

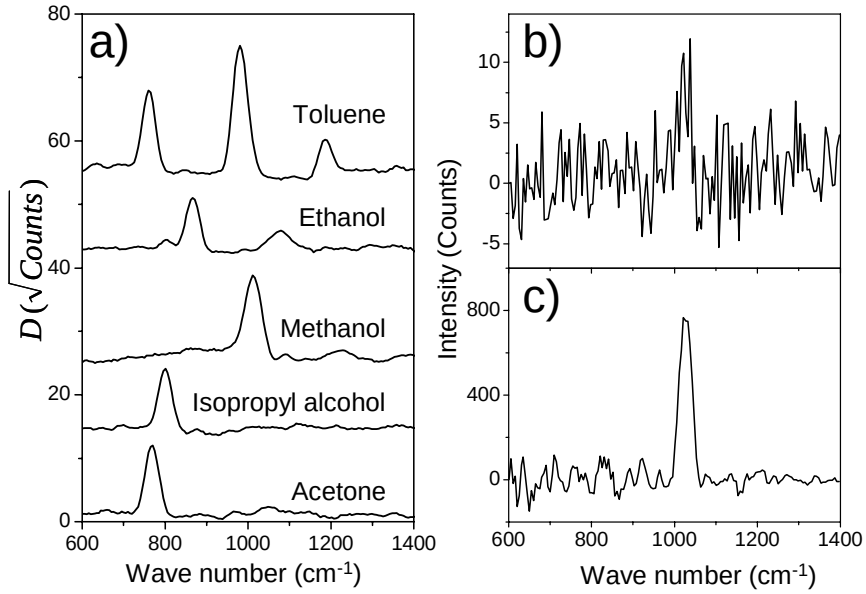
a)
Toluene
Ethanol
Methanol
Isopropyl alcohol
Acetone
$D(\sqrt{Counts})$
Wave number (cm^{-1})
b)
c)
Intensity (Counts)
Wave number (cm^{-1})